Journal of proteome research

Article

pubs.acs.org/jpr

The Presence of Outer Arm Fucose Residues on the *N*-Glycans of Tissue Inhibitor of Metalloproteinases-1 Reduces Its Activity

Han Ie Kim,[†,#,▽] Radka Saldova,[‡,#] Jun Hyoung Park,[†] Young Hun Lee,[†] David J. Harvey,[§] Mark R. Wormald,[§] Kieran Wynne,[∥] Giuliano Elia,[∥] Hwa-Jung Kim,[⊥] Pauline M. Rudd,[‡,*] and Seung-Taek Lee[†,*]

[†]Department of Biochemistry, College of Science and Biotechnology, Yonsei University, Seoul 120-749, Republic of Korea

[‡]NIBRT GlycoScience Group, NIBRT, Mount Merrion, Blackrock, Dublin, Ireland

[§]Department of Biochemistry, Oxford Glycobiology Institute, University of Oxford, Oxford OX1 3QU, U.K.

[∥]The Mass Spectrometry Resource, Conway Institute, UCD, Dublin 4, Ireland

[⊥]School of Pharmacy, Ewha Womans University, Seoul 120-750, Republic of Korea

Supporting Information

ABSTRACT: Tissue inhibitor of metalloproteinases-1 (TIMP-1) inhibits matrix metalloproteinases (MMPs) by binding at a 1:1 stoichiometry. Here we have shown the involvement of *N*-glycosylation in the MMP inhibitory ability of TIMP-1. TIMP-1, purified from HEK 293 cells overexpressing TIMP-1 (293 TIMP-1), showed less binding and inhibitory abilities to MMPs than TIMP-1 purified from fibroblasts or SF9 insect cells infected with TIMP-1 baculovirus. Following deglycosylation of TIMP-1, all forms of TIMP-1 showed similar levels of MMP binding and inhibition, suggesting that glycosylation is involved in the regulation of these TIMP-1 activities. Analysis of the *N*-glycan structures showed that SF9 TIMP-1 has the simplest *N*-glycan structures, followed by fibroblast TIMP-1 and 293 TIMP-1, in order of increasing complexity in their *N*-glycan structures. Further analyses showed that cleavage of outer arm fucose residues from the *N*-glycans of 293 TIMP-1 or knockdown of both FUT4 and FUT7 (which encode for fucosyltransferases that add outer arm fucose residues to *N*-glycans) enhanced the MMP-binding and catalytic abilities of 293 TIMP-1, bringing them up to the levels of the other TIMP-1. These results demonstrate that the ability of TIMP-1 to inhibit MMPs is at least in part regulated by outer arm fucosylation of its *N*-glycans.

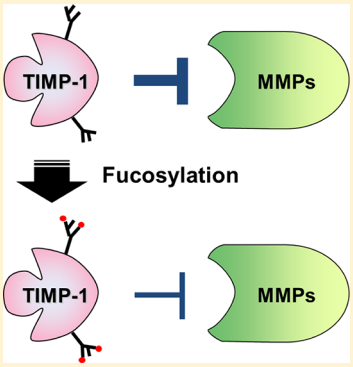

KEYWORDS: *fucosylation, glycosylation, inhibition, MMP, N-glycan, TIMP-1*

INTRODUCTION

Tissue inhibitors of matrix metalloproteinases (TIMPs) inhibit the proteolytic activity of matrix metalloproteinases (MMPs) by binding to MMPs with 1:1 stoichiometry.[1] Inhibition of MMPs by TIMPs is accomplished by coordination of the Zn^{2+} ion of the MMP active site with the amino and carbonyl groups of N-terminal cysteine residues of each TIMP.[2,3] MMPs degrade various components of an extracellular matrix and are involved in normal physiological processes such as wound repair and in many pathological processes, including tumor invasion, metastasis, arthritis, and inflammation. TIMP-mediated MMP inhibition is thought to alleviate these damaging processes.[4,5]

Glycosylation is one of the most common posttranslational modifications. Glycoproteins are proteins that are modified by the attachment of a heterogeneous collection of sugars at each glycosylation site. Glycan-processing pathways are complex and reflect the environment both inside and outside of the cells. These pathways can be changed in normal physiological and pathological situations. Glycosylation alterations resulting from changes to glycan-processing pathways can often modulate the biological functions of physiologically important proteins.[6]

Among the four types of TIMPs, TIMP-1 and TIMP-3 carry *N*-glycans. TIMP-1 inhibits the majority of soluble MMPs, including MMP-1, MMP-2, MMP-3, MMP-7, and MMP-9, but it does not inhibit most of the membrane-type MMPs, such as MMP-14, MMP-15, MMP-16, and MMP-24.[7,8] The N- and C-terminal domains of TIMP-1 have different functions. The N-terminal domain, corresponding to residues 1−126 in humans, is important in the inhibition of MMPs. Oligosaccharide chains are attached at two asparagine residues in the N-terminal domain: Asn30, between the first and second β sheets, and Asn78, between the third and fourth β sheets.[9,10] It was reported that removal of these *N*-glycans, either singly or in combination, reduces protein stability but does not affect its MMP-inhibitory activity, implying the lack of involvement of glycosylation in this process.[11] However, more recently, Kim et al. reported that overexpression of *N*-acetylglucosaminyltrans-

Received: February 21, 2012
Published: June 14, 2013

ferase (GnT)-V gives rise to aberrant glycosylation, including addition of β1,6-*N*-acetylglucosamine (β1,6-GlcNAc), of TIMP-1, in colon cancer WiDr cells and that the aberrantly glycosylated TIMP-1 showed weaker inhibition of MMP-2 and 9 and higher metastatic potential than normal TIMP-1.[12] However, the TIMP-1 that was aberrantly glycosylated with β-1,6-GlcNAc was detected at low concentrations of 0.8 ng/mL in serum from colon cancer patients,[13] whereas the levels of normally glycosylated TIMP-1 in serum from colon cancer patients reached 100−700 ng/mL.[14−16] Therefore, it remains to be elucidated whether aberrant *N*-glycan modifications on TIMP-1 are involved in the reduction of the MMP inhibitory activity and the enhancement of metastasis in colon cancer patients.

In the current study, it was determined whether the differential *N*-glycosylation of TIMP-1 affects its MMP binding ability and/or inhibitory property. TIMP-1 variants, purified from various cell types, were examined: SF9 TIMP-1 from SF9 cells infected with TIMP-1 baculovirus; fibroblast (FBB) TIMP-1 from human foreskin fibroblasts; and 293 TIMP-1 from HEK 293 cells that overexpress TIMP-1. An ELISA-based assay was developed to analyze the interaction of TIMP-1 and MMPs. Glycosylated and deglycosylated TIMP-1 samples were tested for their abilities to bind to MMP along with their abilities to inhibit MMP. The glycosylation profiles of the TIMP-1 types were determined using hydrophilic interaction liquid chromatography (HILIC)-based glycoanalytical technology. Further investigations were carried out on the form of TIMP-1 that showed reduced MMP binding ability, and a sugar modification and certain glycosyltransferases were identified as being crucial in this process. Knockdowns of the glycosyltransferases of interest were generated, and the results demonstrate that altered glycosylation of TIMP-1 can reduce its MMP inhibitory function.

MATERIALS AND METHODS

Construction of TIMP-1 Expression Vector

The human full-length TIMP-1 cDNA was amplified by PCR using a primer pair, 5′-CCC*AAGCTT*CCAGAGAACCCAC-**CATG**GCC-3′ (nt. 179−198 of GenBank NM_003254 is underlined, a HindIII site is italicized, and a translation initiating codon is bold-faced) and 5′-CG*GGATCC***TCA**GGC-TATCTGGGACCGCA-3′ (nt. 816−797 of GenBank NM_003254 is underlined, a BamHI site is italicized, and a termination codon is bold-faced) and pGEM-T-TIMP-1[17] as template. A human TIMP-1 expression vector, pcDNA3.1-TIMP-1, was constructed by subcloning of the 644-bp HindIII-BamHI fragment of the full-length human TIMP-1 cDNA into the same sites of the pcDNA3.1 vector (Invitrogen, Carlsbad, CA). The final construct was sequenced to avoid PCR errors.

Cell Culture and Cell Lines

Human foreskin fibroblast cells (Welskin, Seoul, Republic of Korea) and HEK 293 cells were cultured in Dulbecco's modified Eagle's medium (GIBCO BRL, Grand Island, NY) supplemented with 5% FBS, 100 units/mL penicillin, and 0.1 mg/mL streptomycin at 37 °C. An HEK 293 cell line stably expressing TIMP-1 (293-TIMP-1) was generated by transfection of HEK 293 cells with pcDNA3.1-TIMP-1 by the calcium phosphate method, followed by selection with 1200 μg/mL G418.[18,19]

Knockdown of FUT4 and FUT7 in HEK 293 Cells

shRNA constructs for fucosyltransferase-4 (FUT4) and fucosyltrasferase-7 (FUT7) (MISSON TRC shRNA, Sigma-Aldrich, St. Louis, MO) were screened for the ability to knockdown their expression. shRNA constructs that efficiently decreased expression of FUT4 and FUT7 were transfected into 293-TIMP-1 cells using the calcium phosphate method and selected with 1 μg/mL of puromycin to generate shFUT4 293-TIMP-1 or shFUT7 293-TIMP-1 cell line, respectively.

Preparation of TIMP-1

SF9 TIMP-1 was expressed from SF9 insect cells infected with human TIMP-1 baculovirus as described previously.[17,20] TIMP-1 variants from foreskin fibroblasts, 293-TIMP-1 cells, shFUT4 293-TIMP-1 cells, and shFUT7 293-TIMP-1 cells, were purified by using TIMP-1 monoclonal antibody (mAb) affinity resin. The serum-free conditioned medium (1 L) was subjected to ammonium sulfate precipitation with 80% saturation. The pellet was dissolved in 20 mL of PBS (137 mM NaCl, 10 mM Na_2HPO_4, 2.7 mM KCl, and 2 mM KH_2PO_4, pH 7.4) containing 1 mM phenylmethanesulfonyl fluoride (PMSF) and loaded onto an anti-TIMP-1 monoclonal antibody-conjugated Sepharose column (0.5 mL of bed volume) equilibrated in PBS. TIMP-1 was eluted with 0.1 M glycine-HCl, pH 2.5. The collected fractions were dialyzed into MMP reaction buffer (20 mM Tris−HCl, pH 7.5, 150 mM NaCl, 5 mM $CaCl_2$, 500 μM $ZnCl_2$, 0.001% Brij-35). For the analysis of the *N*-glycans of TIMP-1, TIMP-1 variants were purified by serial column chromatography. The conditioned media (1 L) were loaded onto a Q-Sepharose FF column (10 mL of bed volume) (GE Healthcare, Piscataway, NJ) equilibrated with 20 mM Tris-HCl, pH 7.4. Proteins in the flow-through fraction were precipitated by 80% ammonium sulfate and resuspended in 20 mM Tris-HCl, pH 7.4. The resuspended sample was loaded onto a heparin-Sepharose FF column (2 mL of bed volume) (GE Healthcare) equilibrated with 20 mM Tris-HCl, pH 7.4, and the bound protein was eluted with a linear gradient of 0−1 M NaCl. The active fractions were loaded onto a ConA Sepharose 4B column (0.5 mL of bed volume) (GE Healthcare) equilibrated with 20 mM Tris-HCl, pH 7.4, and 0.5 M NaCl, and the bound protein was eluted with a linear gradient of buffer containing 0.02−0.2 M α-D-methylmannoside. The active fractions were dialyzed against MMP reaction buffer. All purification steps were performed at 4 °C. Proteins were quantified with a Micro BCA Protein Assay Reagent kit (Pierce, Rockford, IL) and were confirmed by MS/MS analysis of tryptic peptides using a Thermo Scientific LTQ ORBITRAP XL mass spectrometer. Spectra were matched against a redundant human Swissprot database using the algorithm TurboSEQUEST.

Deglycosylation of TIMP-1

TIMP-1 was deglycosylated by incubating with 0.2 μg peptide *N*-glycosidase F (PNGase-F)/μg TIMP-1 in 20 mM Tris-HCl (pH 7.4) for 24 h at 37 °C.[21]

Preparation of MMPs

The catalytic domain of human MMP-3 (cMMP-3, Phe100-Pro273), the pro, catalytic, and hinge domains of human MMP-1 (pchMMP-1, Phe20-Ala277), and the catalytic and hinge domains of human MMP-14 (cMMP-14, Tyr112-Ile318) were expressed as inclusion bodies in *E. coli* and were purified using a previously reported refolding method.[22] Immediately prior to use, the pchMMP-1 was activated to cMMP-1 by incubation

dx.doi.org/10.1021/pr400276r | J. Proteome Res. 2013, 12, 3547−3560

with 1 mM 4-aminophenyl mercuric acetate (APMA) for 1 h at 37 °C.[23]

ELISA-Based MMP/TIMP-1 Binding Assay

96-well plates (650 061, Greiner, Monroe, NC) coated with cMMP-3, cMMP-1, or cMMP-14 (1 μg/well) were incubated at 4 °C overnight and were blocked with 1% BSA in Tris-buffered saline (20 mM Tris-HCl pH 7.4, 150 mM NaCl) for 1 h at 37 °C. Various concentrations of TIMP-1 in MMP reaction buffer were added to the wells and incubated for 2 h at 37 °C. To detect TIMP-1 bound to MMP, anti-TIMP-1 antibody (Ab-1; 1:5000, Calbiochem, Darmstadt, Germany), horseradish peroxidase-conjugated antimouse IgG antibody, and 3,3′,5,5′-tetramethylbenzidine substrate (Sigma) were sequentially reacted and absorbance was then measured at 450 nm.

Electrophoresis and Western Blot Analysis

Prior to electrophoresis, all samples were reduced with 5% 2-mercaptoethanol. Electrophoresis was performed in sodium dodecyl sulfate (SDS) PAGE mini-gels buffered with Tris-Glycine for analysis of TIMP-1 and fucosyltransferases or buffered with Tris-Tricine for analysis of α-synuclein at room temperature according to the method of Laemmli.[24] The gels were stained with Coomassie brilliant blue (CBB) R-250. For Western blot analysis, proteins in gels were transferred to nitrocellulose or PVDF membrane (Millipore Corp., Beford, MA). Immunoreactive proteins were visualized with anti-TIMP-1, anti-MMP-3 (AF513; R&D, Minneapolis, MN), anti-FUT4 (sc-14871; Santa Cruz Biotechnologies, Santa Cruz, CA), anti-FUT7 (AT2124a; ABGENT, San Diego, CA), and antiglyceraldehyde-3-phosphate dehydrogenase (GAPDH) (LF-PA0018; AbFrontier, Seoul, Republic of Korea) primary antibodies, horseradish peroxidase-conjugated secondary antibody, and an enhanced chemiluminescent detection kit (GE Healthcare).

Fluorogenic Peptide Cleavage Assay with cMMP-3 in the Presence of TIMP-1

cMMP-3 (10 nM) was incubated in 100 μL of the MMP reaction buffer containing 1 μM of a quenched fluorescent peptide ((7-methoxycoumarin-4-yl)acetyl-Arg-Pro-Lys-Pro-Tyr-Ala-Nva-Tyr-Met-Lys(2,4-dinitrophenyl)-NH_2; M2105, Bachem, Torrance, CA) as a substrate in the absence or presence of TIMP-1 (1:0.5, 1:1, 1:2 molar ratio of cMMP-3/TIMP-1) for 10 min at 37 °C. The fluorescence was measured at an excitation wavelength of 328 nm and an emission wavelength of 393 nm.

Cleavage of α-Synuclein with cMMP-3 in the Presence of TIMP-1

α-Synuclein (1 μg, ATGen, Seongnam, Republic of Korea) was digested with cMMP-3 in a 1:10 enzyme/substrate molar ratio in 10 μL of MMP reaction buffer for 30 min at 37 °C[25] in the presence of TIMP-1 (1:1 enzyme/inhibitor molar ratio). Reactions were stopped by the addition of SDS sample buffer. Each sample was subjected to 15% Tris-Tricine gel and stained with CBB R-250.

Purification and Fluorescent Labeling of *N*-Glycans from TIMP-1

N-Glycans were released from TIMP-1 within a block of SDS-gel by *in situ* digestion with PNGase F (Roche, Mannheim, Germany) as described earlier.[26] The *N*-glycans for HILIC analysis were fluorescently labeled with 2-aminobenzamide (2AB) by reductive amination[27] (LudgerTag 2-AB Glycan Labeling kit, Ludger Ltd., Abingdon, U.K.).

Exoglycosidase Digestion of 2AB Labeled *N*-Linked Glycans

All enzymes were purchased from Glyko (Novato, CA) or New England Biolabs (Hitchin, Herts, U.K.). The 2AB-labeled glycans were digested in a volume of 10 μL for 18 h at 37 °C in 50 mM sodium acetate buffer, pH 5.5, using arrays of the following enzymes: ABS, *Arthrobacter ureafaciens* sialidase (EC 3.2.1.18), 1 U/mL; NAN1, *Streptococcus pneumoniae* sialidase (EC 3.2.1.18), 1 U/mL; BTG, bovine testes β-galactosidase (EC 3.2.1.23), 1 U/mL; SPG, *Streptococcus pneumoniae* β-galactosidase (EC 3.2.1.23), 0.1 U/mL; BKF, bovine kidney α-fucosidase (EC 3.2.1.51), 1 U/mL; GUH, β-*N*-acetylglucosaminidase cloned from *Streptococcus pneumonia*, expressed in *E. coli* (EC 3.2.1.30), 4 U/mL; JBH, jack bean β-*N*-acetylhexosamidase or acetylhexos-amindase (EC 3.2.1.24), 50 U/mL; AMF, almond meal α-fucosidase (EC 3.2.1.111), 3 mU/mL; XMF, *Xanthomonus sp.* α-fucosidase (EC 3.2.1.51), 0.1 U/mL. After incubation, enzymes were removed by filtration through a protein-binding EZ filter (Millipore Corporation, Beford, MA);[26] the *N*-glycans were then analyzed by HILIC.

Hydrophilic Interaction Liquid Chromatography (HILIC)

HILIC was performed using a TSK-Gel Amide-80 4.6 mm × 250 mm column (Anachem, Luton, U.K.) on a 2695 Alliance separations module (Waters, Milford, MA) with a Waters temperature control module and a Waters 2475 fluorescence detector. Solvent A was 50 mM formic acid (pH 4.4 with ammonia solution). Solvent B was acetonitrile. The column temperature was set to 30 °C, and a linear gradient of 20−58% A over 152 min at a flow rate of 0.4 mL/min was employed. Samples were injected in 80% acetonitrile.[28] Fluorescence was measured at an emission wavelength of 420 nm with excitation at 330 nm. The system was calibrated using an external standard of hydrolyzed and 2AB-labeled glucose oligomers to create a dextran ladder, as described previously.[26]

MALDI-TOF MS

Positive ion MALDI-TOF mass spectra of the SF9 TIMP-1 and 293 TIMP-1 *N*-glycans were recorded with a Micromass TofSpec 2E reflectron-TOF mass spectrometer (Waters MS Technologies, Manchester, U.K.) fitted with delayed extraction and a nitrogen laser (337 nm). The acceleration voltage was 20 kV; the pulse voltage was 3.2 kV; the delay for the delayed extraction ion source was 500 ns. MALDI-TOF spectra of the FBB TIMP-1 *N*-glycans were recorded with a Waters Micro MX MALDI-TOF mass spectrometer in reflectron mode with an acceleration voltage of 12 kV. Samples were cleaned with a Nafion 117 membrane[29] and were prepared for MALDI analyzis by depositing 0.5 μL of the sample solution onto the stainless steel target plate, adding 0.3 μL of the matrix solution (a saturated solution of 2,5-dihydroxybenzoic acid in acetonitrile), and allowing the mixture to dry at room temperature. The sample/matrix mixture was then recrystallized from ethanol.[30]

Negative Ion Electrospray Ionization Mass Spectrometry ESI-MS and ESI MS/MS

Nanoelectrospray mass spectrometry was performed with a Waters quadrupole (Q)-TOF Ultima Global instrument. Samples in 1:1 (v/v) methanol/water containing 0.5 mM ammonium phosphate were infused through Proxeon (Proxeon Biosystems, Odense, Denmark) nanospray capillaries. The ion source conditions were as follows: temperature, 120 °C; nitrogen flow, 50 L/h; infusion needle potential, 1.2 kV; cone

dx.doi.org/10.1021/pr400276r | J. Proteome Res. 2013, 12, 3547−3560

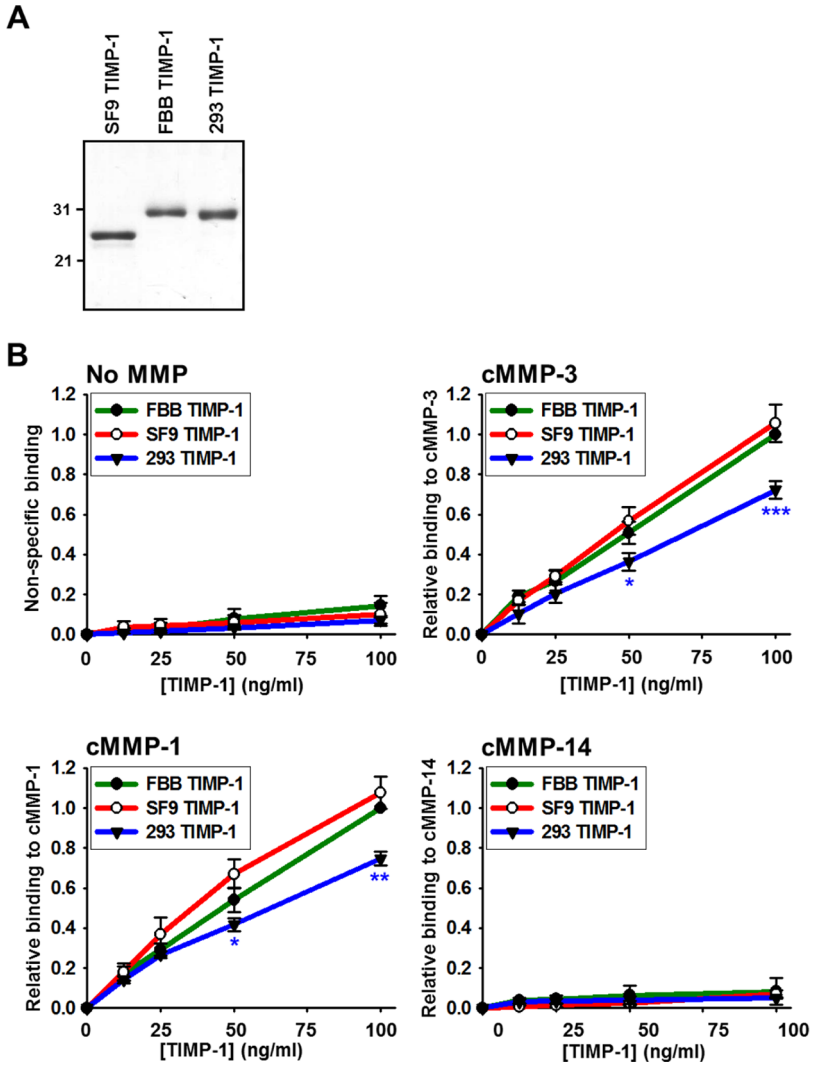

Figure 1. Purification of TIMP-1 variants and their binding to MMPs. (A) SDS-PAGE of the TIMP-1 variants. The purified TIMP-1 variants, SF9 TIMP-1, FBB TIMP-1, and 293 TIMP-1, were subjected to SDS-PAGE. (B) Binding of TIMP-1 variants to MMPs analyzed with an ELISA-based assay. FBB TIMP-1 (green line), SF9 TIMP-1 (red line), and 293 TIMP-1 (blue line) were assayed by an ELISA-based method to measure background binding (no MMP) or binding to cMMP-3, cMMP-1, or cMMP-14. Values represent the mean ± SD of three independent determinations. Statistical comparison was performed by Student's *t* test and referred to the binding of FBB TIMP-1 to MMPs. *, $p < 0.05$; **, $p < 0.01$; ***, $p < 0.005$.

voltage, 100 V; RF-1 voltage, 150 V. Spectra (2 s scans) were acquired with a digitization rate of 4 GHz and accumulated until a satisfactory signal/noise ratio had been obtained. For MS/MS data acquisition, the parent ion was selected at low resolution (about 4 m/z mass window) to allow transmission of isotope peaks and fragmented with argon. The voltage on the collision cell was adjusted with mass and charge to give an even distribution of fragment ions across the mass scale. Typical values were 80−120 V.

Exoglycosidase Digestion of *N*-Glycans of TIMP-1 for the MMP-3/TIMP-1 Binding Assay

N-Glycans of TIMP-1 (2 μg) were digested for 24 h at 37 °C in 50 mM sodium acetate buffer, pH 5.5, using exoglycosidases, ABS, JBH, BTG, AMF, BKF, and GUH. The exoglycosidase-digested TIMP-1 was neutralized with 0.1 M Tris-HCl, pH 8.0, in a final concentration.

Reverse Transcription (RT)-PCR

Total RNA was isolated using TRIzol reagent (Invitrogen) according to the manufacturer's recommendations. RT-PCR was performed as detailed previously.[31] The primer pair sequences for PCR amplification of human FUT cDNAs[32−34] were shown in Supporting Information Table 1.

Molecular Modeling

Molecular modeling was performed on a Silicon Graphics Fuel workstation using InsightII and Discover software (Accelrys Inc., San Diego, CA). Figures were produced using the program MolScript.[35] The molecular model of MMP-3/TIMP-1 was based on the crystal structure of the human complex[36] obtained from the PDB database.[37] *N*-Linked glycan structures, chosen on the basis of sequencing results, were generated using the database of glycosidic linkage conformations[38] and *in vacuo* energy minimization to relieve unfavorable steric interactions. The Asn-GlcNAc linkage conformations were based on the observed range of crystallographic values,[39] with the torsion angles around the Asn Cα-Cβ and Cβ-Cγ bonds then being adjusted to eliminate unfavorable steric interactions between the glycans and the protein surface.

dx.doi.org/10.1021/pr400276r | *J. Proteome Res.* 2013, 12, 3547−3560

RESULTS

293 TIMP-1 Exhibits Reduced Binding to and Inhibition of MMPs

To investigate the ability of TIMP-1 to bind to and inhibit MMPs, TIMP-1 variants purified from various cell types were examined: SF9 TIMP-1 from SF9 cells infected with TIMP-1 baculovirus; FBB TIMP-1 from human foreskin fibroblasts; and 293 TIMP-1 from HEK 293 cells that overexpress TIMP-1. Figure 1A shows that the apparent molecular weight of SF9 TIMP-1 is approximately 26 kDa and that FBB TIMP-1 and 293 TIMP-1 have higher apparent molecular weights of approximately 30 kDa and 29 kDa, respectively.

TIMP-1 is known to bind to and inhibit most of the soluble MMPs, including MMP-1, -2, -3, -7, and -9.[40] In order to measure the MMP binding ability of the various forms of TIMP-1 in the current study, an ELISA-based MMP/TIMP-1 binding assay was performed using cMMP-1, cMMP-3, and cMMP-14, that were proven to be catalytically active (Supporting Information Figure 1). Under our experimental conditions, the TIMP-1 variants did not bind to uncoated wells. Binding of SF9 TIMP-1 to cMMP-3 or cMMP-1 was very similar to that of FBB TIMP-1, which was used as a normal TIMP-1 control (Figure 1B). However, 293 TIMP-1 exhibited significantly reduced MMP binding to approximately 70% of the level of the MMP binding of FBB TIMP-1 (Figure 1B). TIMP-1 is known not to bind MMP-14.[41] Consistently, the TIMP-1 variants did not bind cMMP-14 used as a negative control (Figure 1B).

Inhibition of the MMP-3 catalytic activity by TIMP-1 was analyzed with a fluorogenic peptide cleavage assay and by cleavage of α-synuclein, which is a protein substrate of MMP-3.[25] The results from the fluorogenic peptide cleavage assay showed that 293 TIMP-1 had a lower inhibitory effect on cMMP-3 than the other TIMP-1 variants (Figure 2A). The digestion of α-synuclein by cMMP-3 was inhibited by SF9 TIMP-1 and FBB TIMP-1 but was inhibited less in the presence of 293 TIMP-1 at a statistically significant level compared to the other TIMP-1 (Figure 2B). These results demonstrate that 293 TIMP-1 has a lower ability to inhibit and to bind to MMP-3 than the other TIMP-1 variants.

Removal of *N*-Glycans Restores the MMP-Inhibiting Ability of 293 TIMP-1

Considering the observation that TIMP-1 is a glycosylated protein, investigations were carried out on the potential involvement of the *N*-glycans on TIMP-1 in its reduced ability to inhibit MMP. Following the removal of the *N*-glycans from the TIMP-1 variants with PNGase-F, the resulting molecular weights for all proteins were found to be approximately 22 kDa, suggesting that the apparent molecular weight of glycosylated 293 TIMP-1 differs from other TIMP-1 variants because of its *N*-glycan content (Figure 3A). Figure 3B shows that the deglycosylated forms of the TIMP-1 variants bind with increased affinity to MMP-3 than the glycosylated form of FBB TIMP-1, implying that the presence of *N*-glycans in TIMP-1 plays a negative role in this binding process. More importantly, deglycosylated 293 TIMP-1 had similar cMMP-3 binding and inhibitory activities as the other deglycosylated TIMP-1 variants (Figure 3B and C). Therefore, *N*-glycosylation appears to be involved in the impaired ability of 293 TIMP-1 to inhibit MMPs.

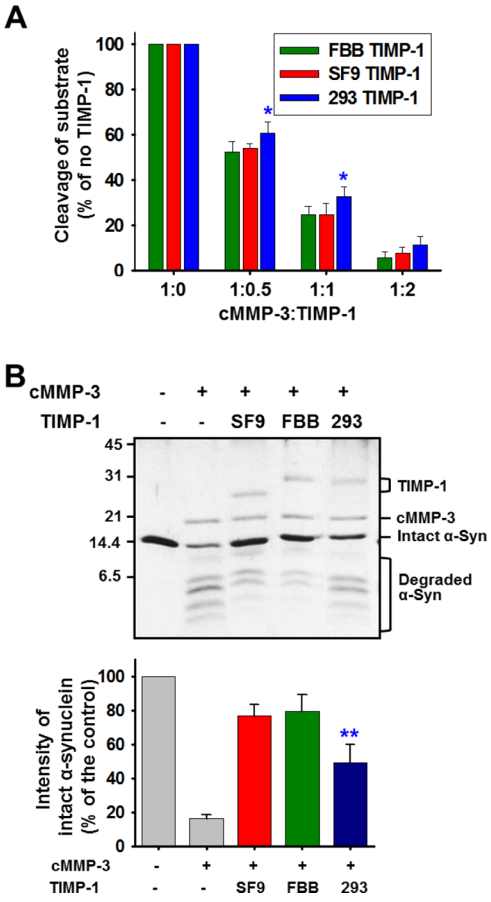

Figure 2. Effects of TIMP-1 variants on the MMP-3 catalytic activity. (A) Fluorogenic peptide cleavage by cMMP-3. The catalytic activity of cMMP-3 was assayed using a fluorogenic peptide in the presence of FBB TIMP-1 (green bars), SF9 TIMP-1 (red bars), and 293 TIMP-1 (blue bars) in 1:0, 1:0.5, 1:1, and 1:2 molar ratios of cMMP-3 and TIMP-1. Data are shown as percentages of the cMMP-3 catalytic activity in the absence of TIMP-1 (mean ± SD, $n \geq 3$). Statistical comparison was shown, which referred to the inhibition of cMMP-3 by FBB TIMP-1. *, $p < 0.05$. (B) Cleavage of α-synuclein by cMMP-3 in vitro. α-Synuclein (1 μg) was digested with cMMP-3 (1:10 enzyme/substrate molar ratio) in the presence of one of the TIMP-1 variants in a 1:1 cMMP-3/TIMP-1 molar ratio. An example of the stained SDS gel is shown in the upper panel. The intact α-synuclein remaining after cMMP-3 cleavage in the presence of TIMP-1 variants was shown as percentages of the uncleaved α-synuclein in a graph in the lower panel (mean ± SD, $n \geq 3$). Statistical comparison was shown, which referred to the cMMP-3 cleavage of α-synuclein in the presence of FBB TIMP-1. **, $p < 0.01$.

293 TIMP-1 Exhibits a Complex Glycosylation Pattern Distinct from Other TIMP-1 Variants

The total *N*-glycans that were released from each TIMP-1 variant were analyzed by HILIC fluorescence, combined with exoglycosidase digestions, with structural assignments made using database matching (GlycoBase; glycobase.nibrt.ie) and by MALDI-TOF and negative ion ESI MS/MS.[42−45] The nomenclature of glycans, typical HILIC chromatograms of *N*-glycans, and *N*-glycan compositions of each TIMP-1 are shown in Figure 4A and B and Table 1, respectively. Assignments of *N*-glycan structures on each TIMP-1 are shown in Supporting Information Figure 2. The experimental masses listed in Table 1 were all within 0.1 mass units of the calculated masses. The glycans on SF9 TIMP-1 were found to be mostly core-

dx.doi.org/10.1021/pr400276r | J. Proteome Res. 2013, 12, 3547−3560

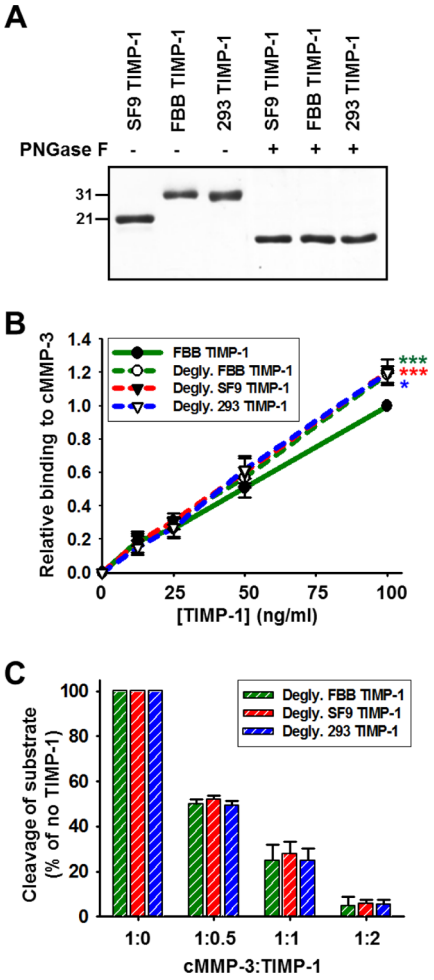

Figure 3. Effects of deglycosylation on MMP-3 binding and inhibition by TIMP-1 variants. (A) Deglycosylation of TIMP-1. The TIMP-1 variants deglycosylated by PNGase-F were subjected to SDS-PAGE. (B) Binding of deglycosylated TIMP-1 variants to cMMP-3 analyzed with an ELISA-based assay. FBB TIMP-1 incubated in deglycosylation buffer (green line) as a normal control, deglycosylated FBB TIMP-1 (dotted green line), deglycosylated SF9 TIMP-1 (dotted red line), and deglycosylated 293 TIMP-1 (dotted blue line) were assayed with an ELISA-based method to measure their cMMP-3-binding abilities. Statistical comparison was shown which referred to the binding of glycosylated FBB TIMP-1 to cMMP-3 (mean ± SD, $n = 3$). *, $p < 0.05$; ***, $p < 0.005$. (C) MMP-3-inhibiting ability of deglycosylated TIMP-1 variants analyzed with a fluorogenic peptide cleavage assay. The cMMP-3 catalytic activity was assayed in the presence of deglycosylated FBB TIMP-1 (striped green bars), deglycosylated SF9 TIMP-1 (striped red bars), and deglycosylated 293 TIMP-1 (striped blue bars) as described above. Data are shown as percentages of the cMMP-3 catalytic activity in the absence of TIMP-1 (mean ± SD, $n \geq 3$).

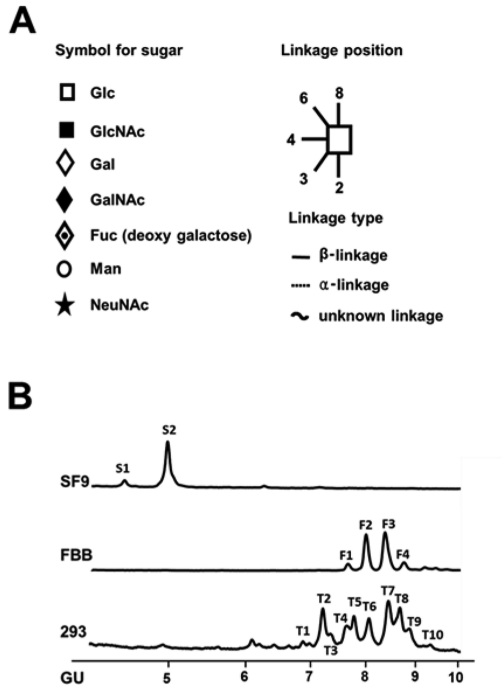

Figure 4. *N*-glycan structure of the TIMP-1 variants. (A) Diagrammatic nomenclature of glycans. Each monosaccharide is represented by a distinct shape and filled to indicate *N*-acetylation. Each line indicates the linkage position at the nonreducing terminus. (B) Typical HILIC chromatograms of *N*-glycans from SF9 TIMP-1, FBB TIMP-1, and 293 TIMP-1. Peak identification and *N*-glycan structure are shown in Table 1.

fucosylated $Man_3GlcNAc_2$ (F(6)M3, see Table 1 for abbreviations) with some M3. FBB TIMP-1 contained mostly core fucosylated biantennary glycans with one or two α2,3-linked sialic acids [F(6)A2G(4)2S(3)1 and F(6)A2G(4)2S(3,3)2], but also biantennary glycans without any sialic acids [F(6)-A2G(4)2 and A2G(3,4,4)3] and monosialylated biantennary glycans with one core fucose and one α1,3-linked outer arm fucose [F(6)A2G(4)2F(3)1S(3)1] (Table 1). 293 TIMP-1 exhibited the most complex glycosylation pattern of the analyzed TIMP-1 variants. All of the glycans on 293 TIMP-1 were found to be core fucosylated, biantennary glycans with galactose or GalNAc residues (confirmed by differential reactivity toward GUH and JBH) on the branches and were unsialylated, monosialylated, or disialylated. In addition, many of the glycans had outer arm fucosylation (confirmed by differential sensitivity to the fucosidases and by negative ion MS/MS), and some contained bisecting GlcNAc residues (confirmed by negative ion MS/MS, Table 1).

MMP-3-Binding Ability of 293 TIMP-1 Increases after Removal of Outer Arm Fucose

In order to identify the sugar(s) that may be responsible for decreasing the MMP-inhibitory ability of 293 TIMP-1, 293 TIMP-1 was treated with exoglycosidases. As shown in Figure 5A, the apparent molecular weight of 293 TIMP-1 gradually decreased after incubation with increasing numbers of exoglycosidases. It was discovered that when 293 TIMP-1 was incubated with a mixture of glycosidases including almond meal α-fucosidase (AMF), the MMP-3-binding ability of 293 TIMP-1 was increased to a level similar to that of FBB TIMP-1 (Figure 5B). Moreover, when 293 TIMP-1 was incubated with AMF alone, the MMP-3-binding ability of 293 TIMP-1 was increased to the same level as that of FBB TIMP-1 , that is, a control level (Figure 5C, top panel), while the MMP-3-binding ability of FBB TIMP-1 was not changed by incubation of AMF (Figure 5C, bottom panel). AMF releases α1,3- and α1,4-linked nonreducing terminal fucose residues.[46] On 293 TIMP-1, core fucosylation occurred through α1,6 linkage to GlcNAc residues whereas outer arm fucosylation mostly occurred through α1,3 linkage to GlcNAc residues (Table 1). From these results, it seems that outer arm α1,3-linked fucosylation is responsible for the reduced MMP-3 inhibition of 293 TIMP-1.

dx.doi.org/10.1021/pr400276r | J. Proteome Res. 2013, 12, 3547−3560

Table 1. Chromatographic and Mass Spectral Properties of the Glycans Found on the TIMP-1 Variants[a]

TIMP-1	Peak	GU	m/z		Abbreviation	Structure	% Area
			MALDI ($[M+Na]^+$)	ESI ($[M+H_2PO_4]^-$)			
SF9 TIMP-1	S1	4.42	-	1007.3	M3	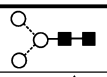	11.7
	S2	4.89	1079.4	1153.4	F(6)M3	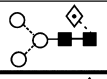	88.4
FBB TIMP-1	F1	7.65	1809.6	1883.5[a]	F(6)A2G(4)2	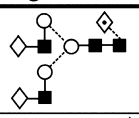	6.9
	F2	8.00	-	2076.6[b]	F(6)A2G(4)2S(3)1	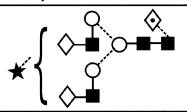	38.3
	F3	8.37	-	1183.4[c]	F(6)A2G(4)2S(3,3)2	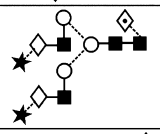	47.9
	F4	8.76	-	-	F(6)A2G(4)2F(3)1S(3)1[d]	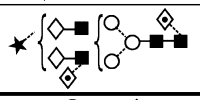	8.0
293 TIMP-1	T1	6.94	1891.7	1965.7	F(6)A2GalNAc2	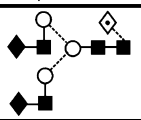	0.40
	T2	7.19	1850.6	1924.6	F(6)A2G(4)1GalNAc[d]	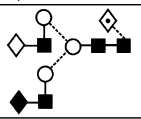	12.8
			1809.6	1883.6	F(6)A2G(4)2	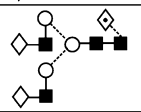	
	T3	7.29	1793.7	1867.6	F(6)M4F(3)1GalNAc1	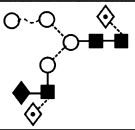	3.9
	T4	7.73	2012.7	2086.7	F(6)A2BG(4)2	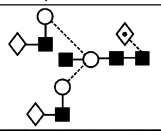	8.8
	T5	7.86	2037.7	2111.7	F(6)A2F(3)1GalNAc2	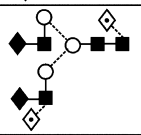	10.3
	T6	8.16	1996.7	2070.6	F(6)A2G(4)1F(3)1GalNAc1	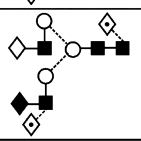	13.2

dx.doi.org/10.1021/pr400276r | J. Proteome Res. 2013, 12, 3547−3560

Table 1. continued

TIMP-1	Peak	GU	m/z MALDI ([M+Na]+)	m/z ESI ([M+H2PO4]-)	Abbreviation	Structure	% Area
	T7	8.41	-	-	F(6)A2G(4)1F(3)1GalNAc1S(3)1	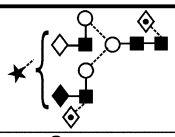	19.7
			2158.8	2232.7	F(6)A2BF(3)1G(4)2	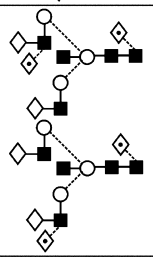	
	T8	8.59	-	-	F(6)A2G(4)2S(6,6)2	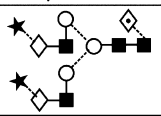	18.5
			-	-	F(6)A2G(4)1GalNAc1S(6,6)2	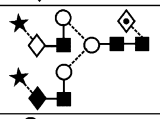	
			1955.7	2029.6	F(6)M5A1F(3)1GalNAc1	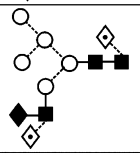	
			2183.7	2257.7	F(6)A2F(3)2GalNAc2	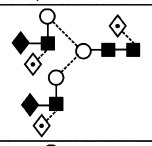	
	T9	8.79	-	-	F(6)A2BG(4)2S2(6,6)2	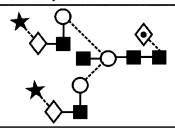	9.5
			2142.9	2216.7	F(6)A2F(3)1G(4)1F(3)1GalNAc1	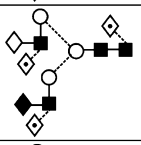	
	T10	9.20	-	2378.8	F(6)A2BF(3)2G(4)2	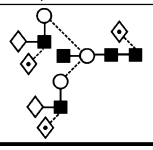	2.9

[a]See Figure 4A for glycan symbols. For further information, see ref 61. Structural abbreviations used: Briefly, all *N*-glycans have two core-*N*-acetylglucosamine (GlcNAc) moieties and a trimannosyl core; F at the start of the abbreviation indicates a core-fucose linked α1,6 to the core-GlcNAc; A[y]a, represents the number of antenna (GlcNAc) on the trimannosyl core-linked to the α1,y mannose arm; B, bisecting GlcNAc linked β1,4 to β1,4 core-mannose; Fb after Aa, represents the number *b* of fucose residues linked α1,3 to antenna GlcNAc; Gc, represents the number *c* of galactose residues linked β1,4 on antenna; GalNAcd represents the number *d* of *N*-acetylglucosamine residues linked β1,4 on antenna; *S*(*z*)*e*, represents the number *e* of sialic acids linked α2,z to the galactose. % Area denotes the relative abundance of each peak from the HILIC chromatogram of *N*-glycans of each TIMP-1. [b]$[M+H_2PO_4]^-$ ion [c]$[M-H]^-$ ion [d]$[M-H_2]^{2-}$ ion [e]Structure not confirmed by fragmentation

N-Glycan Modification by FUT4 and FUT7 Decreases the MMP-3-binding Ability of TIMP-1

A family of α1,3-fucosyltransferases (α1,3-FUTs), including FUT3, 4, 5, 6, 7, and 9, have the ability to add α1,3 fucose residues to GlcNAc residues on the antennae of *N*-glycan.[47,48] In order to identify which α1,3-FUT members are expressed in 293-TIMP-1 cells, an RT-PCR analysis for α1,3-FUT mRNA was performed. 293-TIMP-1 cells exhibited increased expression of FUT4 and FUT7 transcripts when compared to fibroblasts that produce TIMP-1 with very low levels of outer arm α1−3 fucosylation (Figure 6A). Consistent with the RT-PCR data, Western blot analysis showed that FUT4 and FUT7 were expressed at high levels in 293-TIMP-1 cells but they were not detectable in fibroblasts (Figure 6B).

dx.doi.org/10.1021/pr400276r | J. Proteome Res. 2013, 12, 3547−3560

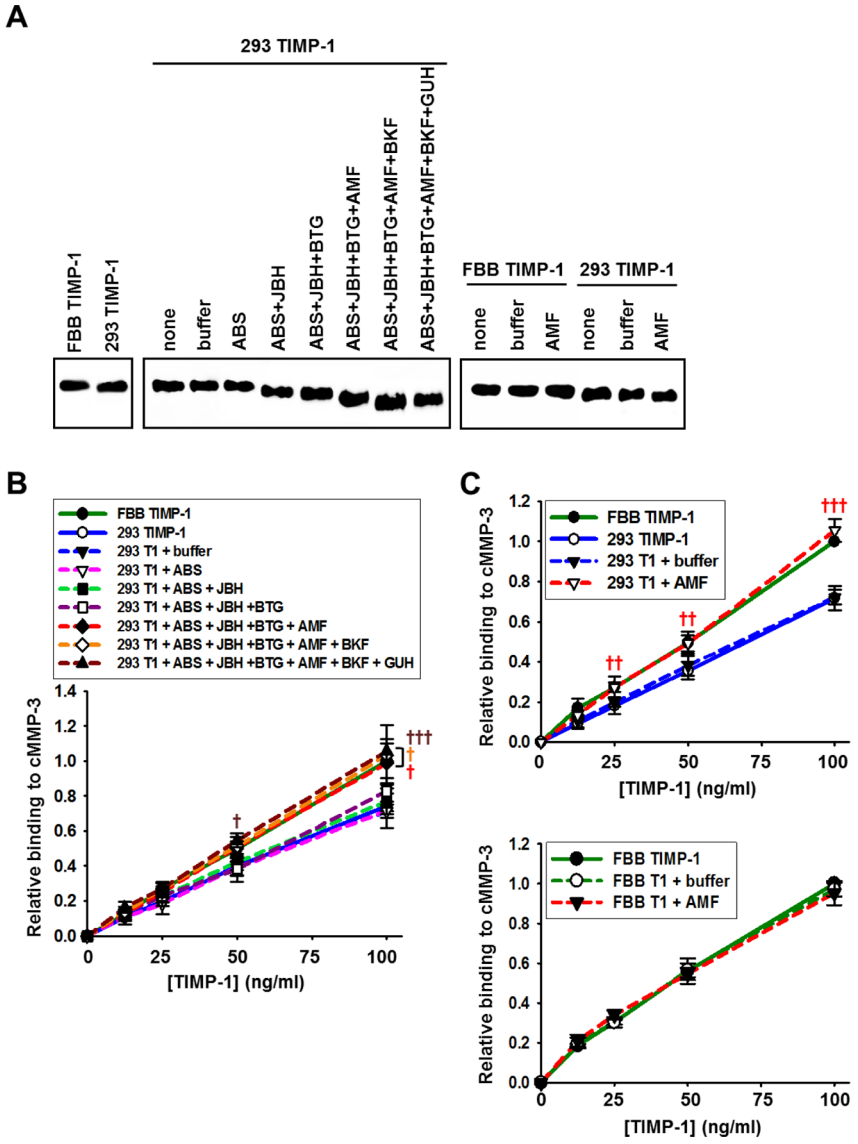

Figure 5. Effects of exoglycosidases on the MMP-3-binding ability of 293 TIMP-1. (A) Digestion of *N*-glycans of 293 TIMP-1 with exoglycosidases. *N*-Glycans of 293 TIMP-1 were digested with arrays of ABS, JBH, BTG, AMF, BKF, and GUH, or with AMF alone with FBB TIMP-1 as a control. The *N*-glycan-digested 293 TIMP-1 was neutralized with 0.1 M Tris-HCl, pH 8.0. Each sample was subjected to SDS-PAGE and Western blot analysis with TIMP-1 antibody. (B) MMP-3 binding of 293 TIMP-1 treated with exoglycosidases. FBB TIMP-1 (green line), 293 TIMP-1 (blue line), 293 TIMP-1 incubated without glycosidases in digestion buffer (dotted blue line), 293 TIMP-1 digested with ABS (dotted pink line), with ABS and JBH (dotted light green line), with ABS, JBH, and BTG (dotted violet line), with ABS, JBH, BTG, and AMF (dotted red line), with ABS, JBH, BTG, AMF, and BKF (dotted orange line), and with ABS, JBH, BTG, AMF, BKF, and GUH (dotted brown line) were assayed by an ELISA-based method to measure binding to cMMP-3. Values represent the mean ± SD of three independent determinations. Statistical comparison was shown, which referred to the binding of 293 TIMP-1 to cMMP-3. †, $p < 0.05$; †††, $p < 0.005$. (C) MMP-3 binding of 293 TIMP-1 digested with AMF. FBB TIMP-1 (green line), 293 TIMP-1 (blue line), 293 TIMP-1 incubated in digestion buffer (dotted blue line), and 293 TIMP-1 digested with AMF (dotted red line) (top panel) and FBB TIMP-1 (green line), FBB TIMP-1 incubated in digestion buffer (dotted green line), and FBB TIMP-1 digested with AMF (dotted red line) (bottom panel) were assayed by an ELISA-based assay for binding to cMMP-3, as described above. Statistical comparison was shown, which referred to the binding of 293 TIMP-1 to cMMP-3 (mean ± SD, $n = 3$). ††, $p < 0.01$; †††, $p < 0.005$.

Knockdown experiments were carried out in order to explore the involvement of FUT4 and FUT7 in the *N*-glycan modification of TIMP-1. shRNA knockdown constructs that decrease expression of FUT4 and FUT7 were screened in HEK 293 cells (Supporting Information Figure 3). Knockdowns of FUT4 and FUT7, individually and together, in 293-TIMP-1 cells were performed by stable transfection of the selected shRNA vectors, and their effectiveness was investigated by Western blotting (Figure 7A). When TIMP-1 variants purified from each cell line were analyzed by SDS-PAGE, all variants showed similar molecular weights (Figure 7B). The MMP-3-binding ability of 293 TIMP-1 increased significantly after knockdown of FUT4 and to a lesser but yet significant extent after knockdown of FUT7 (Figure 7C). Double knockdown of FUT4 and FUT7 increased the MMP-3-binding ability of 293 TIMP-1 to a level similar to that of the FBB TIMP-1 (Figure 7C). Also, the fluorogenic peptide cleavage assay and the α-synuclein digestion analysis revealed that the MMP-3 inhibitory ability of the double knockdown shFUT4/shFUT7 293 TIMP-1 was higher than the control 293 TIMP-1 (Figure 7D and E). These results demonstrate that outer arm α1−3-linked fucosylation, added by the FUT4 and FUT7 enzymes, is

dx.doi.org/10.1021/pr400276r | J. Proteome Res. 2013, 12, 3547−3560

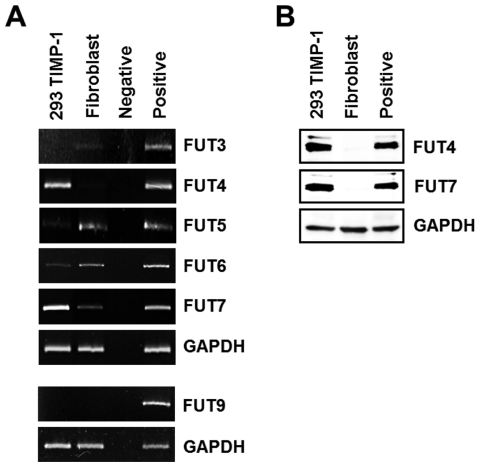

Figure 6. Expression of α1-3 FUTs in 293-TIMP-1 cells and fibroblasts. (A) mRNA levels determined by RT-PCR. cDNA mixtures from 293-TIMP-1 cells and fibroblasts were PCR-amplified with primer pairs for various FUTs. RT-PCR products of GAPDH from the tested cell types were shown to demonstrate that a similar amount of RNA was used in each reaction. Negative control: no DNA. Positive controls: HUVECs in the upper panel or MDAH-2774 cells in the lower panel. (B) Protein levels by Western blotting. The cell lysates were analyzed by Western blot analysis for FUT4, FUT7, and GAPDH. Positive control: HUVECs.

responsible for the decreased binding and inhibitory abilities of 293 TIMP-1.

DISCUSSION

The pathogenesis of many diseases involves modifications to the glycosylation profile of proteins; some examples of these diseases are cancer, congenital disorders of glycosylation, and inflammatory diseases such as rheumatoid arthritis and schizophrenia.[49] For an example, tumor cells often have glycan structures or glycan contents that differ from normal cells.[50,51] These alterations include increased glycan branching by GnTs, increased sialylation and polysialic acid synthesis by sialyltransferases, and the appearance of Lewis-type antigens by fucosyltransferases.[52] Such a subtle change in glycosylation alters protein function and, therefore, can have damaging downstream effects, such as increase of metastatic capacity.

TIMP-1, which is an endogenous inhibitor of MMPs, is a glycoprotein with *N*-linked glycan chains on Asn30 and Asn78.[9] The current study investigates the effects of altered *N*-glycosylation of TIMP-1 on its MMP inhibitory function. TIMP-1 variants, purified from various cell lines, were examined for their abilities to bind to MMPs with an ELISA-based MMP/TIMP-1 binding assay. It was found that the MMP-3 binding ability of 293 TIMP-1 was reproducibly reduced when compared to SF9 TIMP-1 and FBB TIMP-1. Using an ELISA assay, the detection of directly bound TIMP-1 by the TIMP-1 antibody showed that the reduced binding of 293 TIMP-1 to MMP-3 was not due to the difference in the binding of the antibody to TIMP-1 variants (Supporting Information Figure 4). In addition, inhibition of MMP-3 by 293 TIMP-1 was statistically weaker than that by SF9 TIMP-1 and FBB TIMP-1 in both assays using a fluorogenic peptide and α-synclein as a protein substrate. However, the fluorogenic peptide cleavage assay (1:100 enzyme to substrate molar ratio) showed less difference in magnitude than α-synuclein cleavage (1:10 enzyme to substrate molar ratio) probably due to excess molar ratios of the peptide substrate that competes with the inhibitor. Interestingly, the reduction of the MMP binding and the inhibitory activity of the 293 TIMP-1 were abolished, and the MMP binding of all TIMP-1 variants increased, when the *N*-glycans were removed from the protein. These results imply that altered *N*-glycosylation of 293 TIMP-1 is responsible for its reduced binding and inhibition of MMPs.

Glycan analysis of TIMP-1 showed that the *N*-glycosylation patterns of the TIMP-1 variants were significantly different. SF9 TIMP-1 has the simplest *N*-glycan pattern, consisting of M3 and F(6)M3 structures. FBB TIMP-1 contains mostly core fucosylated biantennary glycans with no, one, or two α2−3 linked sialic acids. 293 TIMP-1 shows the most complex glycosylation pattern. The 293 TIMP-1 glycans are core fucosylated, biantennary structures, with galactose or GalNAc on its branches. Some of the glycans are sialylated, and many have outer arm fucosylation.

It was previously shown that the *N*-glycans of TIMP-1 do not affect its MMP-inhibitory activity.[11] However, Kim et al. recently reported that TIMP-1 with *N*-glycans that were modified with β1,6-*N*-acetylglucosamine, due to the over-expression of GnT-V in colon cancer cells, exhibited weaker MMP inhibition than normal TIMP-1, implying a role for glycosylation in the inhibitory activities of TIMP-1.[12] The results in the present study show that 293 TIMP-1, which poorly binds to and inhibits MMPs, does not contain β1,6-*N*-acetylglucosamine in its *N*-glycans. Instead, the presence of abundant outer arm fucosylation on 293 TIMP-1 glycans was found to reduce its binding and inhibitory potential for MMPs.

Fucosylation is one of the common modifications involving oligosaccharides on glycoproteins or glycolipids. Increased levels of fucosylation have been reported under a number of pathological conditions, such as inflammation and cancer.[53] Outer arm fucose is part of Lewis epitopes and is increased in cancer, especially with the formation of metastases, and linked to a poor prognosis.[54,55]

FUT4 preferentially transfers fucose to the inner GlcNAc residue of the polylactosamine chain, while FUT7 cannot transfer fucose to the neutral chain but preferentially transfers fucose to the distal GlcNAc residue of the sialylated polylactosamine chain.[56−58] The *N*-glycans on 293 TIMP-1 have α1−3 fucosylation on the outer arms, which is mostly linked to GlcNAc residues of neutral glycans and partly linked to GlcNAc residues of sialylated glycans. Knockdown of FUT4 exhibited a larger effect on the MMP-binding ability of 293 TIMP-1 than knockdown of FUT7. These results further support our findings that α1,3 fucosylation on the outer arms of *N*-glycans affects the MMP-inhibiting ability of TIMP-1.

The TIMP-1 protein is wedge-shaped, and the broad edge of the protein occupies the active-site cleft of MMP-3.[36] Figure 8 shows models of FBB TIMP-1 with F(6)A2G(4)2S(3,3)2 (see F3 in Table 1 for structure) and 293 TIMP-1 with F(6)A2G(4)1F(3)1GalNAc1S(3)1 (see T7 in Table 1 for structure) attached. The binding of TIMP-1 to MMP-3 induces conformational changes in TIMP-1, including dramatic bending of the AB loop from Glu28 through Leu34, moderate hinge bending of the CD loop between residues Ala65 and Cys70, and modest bending of the Cys1 through Pro6 segment.[36] The bending of the AB loop involves a major change in the backbone torsion angle for each of the residues from Glu28 through Leu34, and contained within this segment is Asn30, one of the *N*-glycosylation sites.[10] The second *N*-linked glycosylation site, Asn78, is not located close to the MMP-

dx.doi.org/10.1021/pr400276r | J. Proteome Res. 2013, 12, 3547−3560

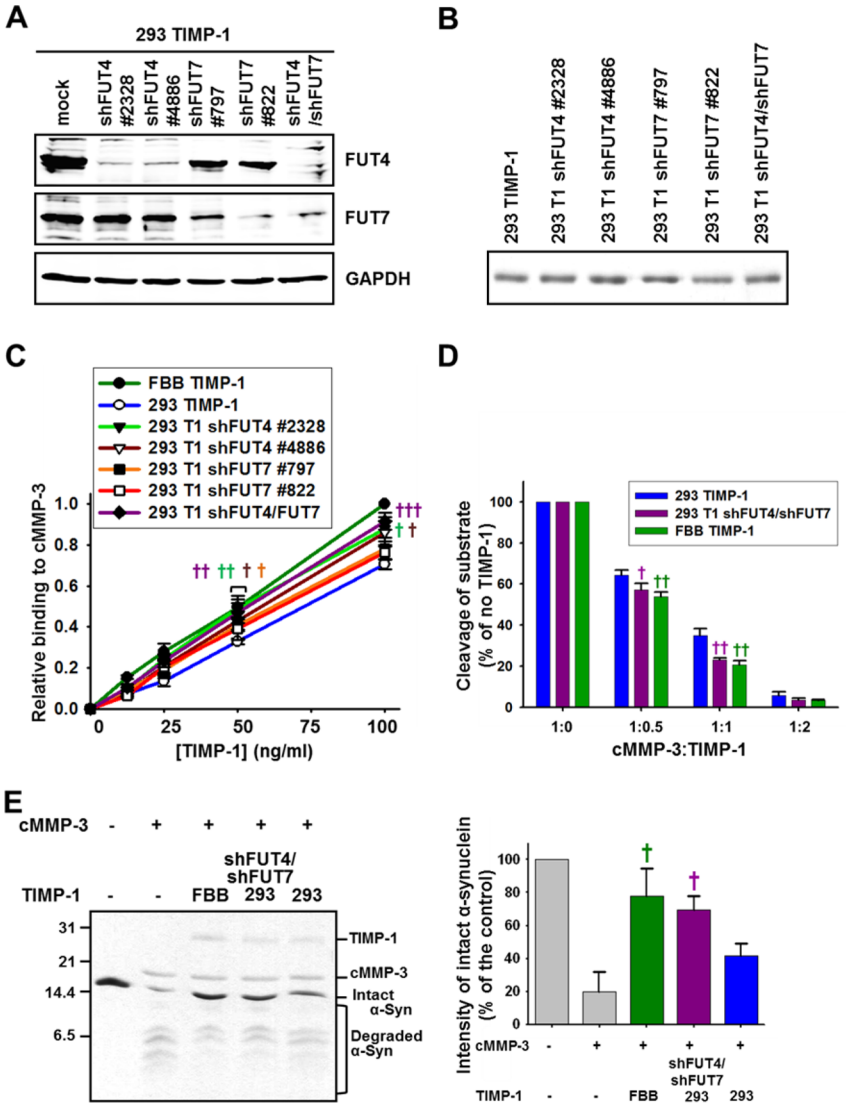

Figure 7. Effects of FUT4 or FUT7 knockdown on MMP-3-binding and inhibition by 293 TIMP-1. (A) Knockdown of FUT4 and FUT7 in HEK 293-TIMP-1 cells. Knockdown was done by stable transfection of shRNA vectors: #2328 and #4886 for FUT4 and #797 and #822 for FUT7. For double knockdown, #2328 FUT4 shRNA vector and #797 FUT7 shRNA vector were used. Expression levels of FUT4 and FUT7 were examined by Western blotting. (B) Purification of TIMP-1 variants from FUT4 and FUT7 knockdown cells. TIMP-1 variants were purified from the serum-free cultured media from FUT4 and FUT7 knockdown 293-TIMP-1 cells and subjected to SDS-PAGE. C) MMP-3 binding of FUT4 and/or FUT7 knockdown TIMP-1. FBB TIMP-1 (green line), 293 TIMP-1 (blue line), 293 TIMP-1 shFUT4 #2328 (light green line), 293 TIMP-1 shFUT4 #4886 (brown line), 293 TIMP-1 shFUT7 #797 (orange line), 293 TIMP-1 shFUT7 #822 (red line), and 293 TIMP-1 shFUT4/shFUT7 (purple line) were assayed by an ELISA-based method to measure binding to cMMP-3. Statistical comparison was shown, referred to the binding of 293 TIMP-1 to cMMP-3 (mean ± SD, $n = 3$). †, $p < 0.05$; ††, $p < 0.01$; †††, $p < 0.005$. (D) MMP-3-inhibiting ability of double FUT4/FUT7 knockdown 293 TIMP-1 analyzed with a fluorogenic peptide cleavage assay. The cMMP-3 catalytic activity was assayed in the presence of 293 TIMP-1 (blue bars), 293 TIMP-1 shFUT4/shFUT7 (purple bars), and FBB TIMP-1 (green bars) as described above. Statistical comparison was shown, which referred to the inhibition of cMMP-3 by 293 TIMP-1 (mean ± SD, $n \geq 3$). †, $p < 0.05$; ††, $p < 0.01$. (E) Effects of double FUT4/FUT7 knockdown on inhibition of cMMP-3-mediated α-synuclein cleavage by TIMP-1. α-Synuclein was digested with cMMP-3 (1:10 enzyme/substrate molar ratio) in the presence of FBB TIMP-1, 293 TIMP-1 shFUT4/shFUT7, and 293 TIMP-1 in a 1:1 cMMP-3/TIMP-1 molar ratio. A typical example of the stained SDS gel is shown in the left panel. Statistical comparison was shown in the right panel, which referred to the cMMP-3 cleavage of α-synuclein in the presence of 293 TIMP-1 (mean ± SD, $n \geq 3$). †, $p < 0.05$.

binding region but in the C-terminal region next to the CD loop. The CD loop covers the wider end of a five-stranded β-barrel and inserts Tyr72 into a hydrophobic pocket formed by the β-barrel.[10] Interestingly, the initial velocity of substrate conversion by MMP-3 in the presence of FBB TIMP-1 showed biphasic kinetics rather than the first order kinetics shown in the absence of TIMP-1 (Supporting Information Figure 5). 293 TIMP-1, containing outer arm fucosylation, also exhibited biphasic kinetics but delayed transition from the rate of the faster component to the rate of the slower component compared to FBB TIMP-1 without outer arm fucosylation. Biphasic kinetics are known to occur in reactions involving an enzyme and slow- and tight-binding inhibitors.[59] Therefore, outer arm fucose residues on the *N*-glycans of Asn30 and Asn78 on TIMP-1, either alone or in combination, may reduce the rate of binding to MMPs by restricting the conformational changes in the MMP-binding region. Additional support for this mechanism comes from the observation that a sialylated

dx.doi.org/10.1021/pr400276r | J. Proteome Res. 2013, 12, 3547−3560

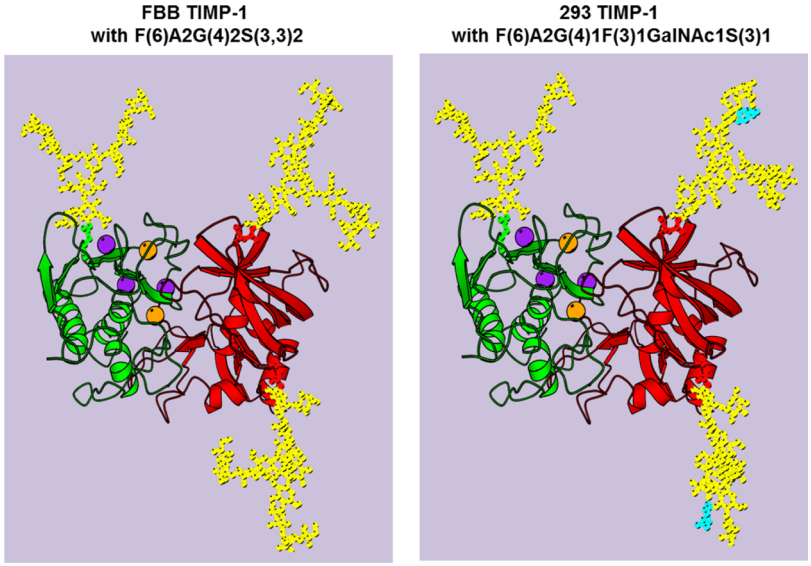

Figure 8. Molecular model of the MMP-3/FBB TIMP-1 complex and the MMP-3/293 TIMP-1 complex. Molecular models show FBB TIMP-1 with F(6)A2G(4)2S(3,3)2 (F3 in Table 1) and 293 TIMP-1 with F(6)A2G(4)1F(3)1GalNAc1S(3)1 (T7 in Table 1) complexed with cMMP-3, based on the protein crystal structure of the human cMMP-3/TIMP-1 complex[36] and the glycan sequencing results. cMMP-3 is shown in green with its *N*-linked glycan in yellow and the bound zinc and calcium ions in orange and purple, respectively. TIMP-1 is shown in red with its *N*-linked glycans in yellow and the outer arm fucose in light blue.

form of MMP-9 was inhibited by TIMP-1 less efficiently than a desialylated form.[60]

In this study, we have shown that 293 TIMP-1 has poorer binding and inhibitory abilities to MMPs than other TIMP-1 variants. The decreased binding and inhibition of 293 TIMP-1 were restored by removal of *N*-glycans from 293 TIMP-1 and, more specifically, by cleavage of outer arm fucoses from the *N*-glycans or silencing of fucosylation enzymes. Our results demonstrate that aberrant glycosylation of TIMP-1, such as fucosylation, could decrease the activities of MMPs. Although the effect of aberrant TIMP-1 glycosylation on MMP activity is not profound, it would result in increased influence on functions of MMP substrates and thus affect the pathophysiology of diseases involving MMPs. Recent advances in the development of glycoanalytical technology have the potential to elucidate aberrant glycan modifications in samples from patients with various diseases, which may be beneficial as molecular markers and therapeutic targets. Therefore, this study would provide a clue for the development of glycan biomarkers as well as the understanding of the mechanism of TIMP-1 inhibition of MMPs.

■ ASSOCIATED CONTENT

Supporting Information

Table of primers and conditions for RT-PCR analysis of α1-3 fucosyltransferase mRNAs; and figures showing catalytic activity assays of cMMP-1, cMMP-3, and cMMP-14; assignments of *N*-glycans released from SF9 TIMP-1, FBB TIMP-1, and 293 TIMP-1; and screening of shRNA vectors for knockdowns of FUT4 and FUT7; comparison of 293 TIMP-1 with FBB TIMP-1 for binding to TIMP-1 antibody; and initial velocity for substrate digestion by MMP-3 in the presence of TIMP-1. This material is available free of charge via the Internet at http://pubs.acs.org.

■ AUTHOR INFORMATION

Corresponding Author

*S.-T.L.: tel, +82-2123-2703; fax, +82-362-9897; e-mail, stlee@yonsei.co.kr. P.M.R.: tel, +353-1215-8142; fax, +353-1215-8116; e-mail, pauline.rudd@nibrt.ie.

Present Address

[∇]H.I.K.: Department of Life Science and Biotechnology, Shingyeong University, Hwaseong, Gyeonggi-do, 445-741, Republic of Korea.

Author Contributions

[#]H.I.K. and R.S. contributed equally to this paper.

Notes

The authors declare no competing financial interest.

■ ACKNOWLEDGMENTS

This study was supported by grants from the National R&D Program for Cancer Control, Ministry of Health and Welfare, Republic of Korea (1120110 to S.-T.L.) and from Studies on Ubiquitome Functions, National Research Foundation, Ministry of Education, Science, and Technology, Republic of Korea (2005-2001143 to S.-T.L.). H.I.K. and J.H.P. were recipients of the postdoctoral trainee program of the Yonsei University Research Fund. Y.H.L. was a predoctoral trainee of the Brain Korea 21 program from Ministry of Education, Science, and Technology, Republic of Korea. R.S. acknowledges funding from the European Union Seventh Framework Programme (FP7/2007-2013) under grant agreement no. 260600 ("GlycoHIT"). Access to and use of the UCD Conway Mass Spectrometry Resource instrumentation is gratefully acknowledged.

■ ABBREVIATIONS

2AB, 2-aminobenzamide; ABS, *Arthrobacter ureafaciens* sialidase; AMF, almond meal α-fucosidase; APMA, 4-aminolphenyl mercuric acetate; BCA, bicinchoninic acid; BKF, bovine kidney

α-fucosidase; BTG, bovine testes β-galactosidase; CBB, Coomassie brilliant blue; ELISA, enzyme-linked immunosorbent assay; ESI, electrospray ionization; FBB, fibroblast; FBS, fetal bovine serum; FUT, fucosyltransferase; GAPDH, glyceraldehyde-3-phosphate dehydrogenase; GnT, *N*-acetylglucosaminyltransferase; GU, glucose units; GUH, β-*N*-acetylglucosaminidase; HEK, human embryonic kidney; HILIC, hydrophilic interaction liquid chromatography; JBH, jack bean α-*N*-acetylhexosaminidase; mAb, monoclonal antibody; MALDI, matrix-assisted laser desorption/ionization; MMP, metalloproteinase; MS, mass spectrometry; NAN1, *Streptococcus pneumoniae* sialidase; PAGE, polyacrylamide gel electrophoresis; PBS, phosphate-buffered saline; PCR, polymerase chain reaction; PMSF, phenylmethanesulfonyl fluoride; PNGase F, peptide *N*-glycosidase F; Q, quadrupole; RT, reverse transcription; SDS, sodium dodecyl sulfate; SPG, *Streptococcus pneumoniae* β-galactosidase; TIMP, tissue inhibitor of metalloproteinases; TOF, time-of-flight; XMF, *Xanthomonus sp.* α-fucosidase

REFERENCES

(1) Tuuttila, A.; Morgunova, E.; Bergmann, U.; Lindqvist, Y.; Maskos, K.; Fernandez-Catalan, C.; Bode, W.; Tryggvason, K.; Schneider, G. Three-dimensional structure of human tissue inhibitor of metalloproteinases-2 at 2.1 A resolution. *J. Mol. Biol.* **1998**, *284* (4), 1133−40.

(2) Murphy, G.; Houbrechts, A.; Cockett, M. I.; Williamson, R. A.; O'Shea, M.; Docherty, A. J. The N-terminal domain of tissue inhibitor of metalloproteinases retains metalloproteinase inhibitory activity. *Biochemistry* **1991**, *30* (33), 8097−102.

(3) Willenbrock, F.; Crabbe, T.; Slocombe, P. M.; Sutton, C. W.; Docherty, A. J.; Cockett, M. I.; O'Shea, M.; Brocklehurst, K.; Phillips, I. R.; Murphy, G. The activity of the tissue inhibitors of metalloproteinases is regulated by C-terminal domain interactions: a kinetic analysis of the inhibition of gelatinase A. *Biochemistry* **1993**, *32* (16), 4330−7.

(4) Brew, K.; Dinakarpandian, D.; Nagase, H. Tissue inhibitors of metalloproteinases: evolution, structure and function. *Biochim. Biophys. Acta* **2000**, *1477* (1−2), 267−83.

(5) Gomez, D. E.; Alonso, D. F.; Yoshiji, H.; Thorgeirsson, U. P. Tissue inhibitors of metalloproteinases: structure, regulation and biological functions. *Eur. J. Cell Biol.* **1997**, *74* (2), 111−22.

(6) Hakomori, S. Tumor malignancy defined by aberrant glycosylation and sphingo(glyco)lipid metabolism. *Cancer Res.* **1996**, *56* (23), 5309−18.

(7) Baker, A. H.; Edwards, D. R.; Murphy, G. Metalloproteinase inhibitors: biological actions and therapeutic opportunities. *J. Cell Sci.* **2002**, *115* (Pt 19), 3719−27.

(8) Stetler-Stevenson, W. G. Tissue inhibitors of metalloproteinases in cell signaling: metalloproteinase-independent biological activities. *Sci. Signal* **2008**, *1* (27), re6.

(9) Carmichael, D. F.; Sommer, A.; Thompson, R. C.; Anderson, D. C.; Smith, C. G.; Welgus, H. G.; Stricklin, G. P. Primary structure and cDNA cloning of human fibroblast collagenase inhibitor. *Proc. Natl. Acad. Sci. U.S.A.* **1986**, *83* (8), 2407−11.

(10) Wu, B.; Arumugam, S.; Gao, G.; Lee, G. I.; Semenchenko, V.; Huang, W.; Brew, K.; Van Doren, S. R. NMR structure of tissue inhibitor of metalloproteinases-1 implicates localized induced fit in recognition of matrix metalloproteinases. *J. Mol. Biol.* **2000**, *295* (2), 257−68.

(11) Caterina, N. C.; Windsor, L. J.; Bodden, M. K.; Yermovsky, A. E.; Taylor, K. B.; Birkedal-Hansen, H.; Engler, J. A. Glycosylation and NH2-terminal domain mutants of the tissue inhibitor of metalloproteinases-1 (TIMP-1). *Biochim. Biophys. Acta* **1998**, *1388* (1), 21−34.

(12) Kim, Y. S.; Hwang, S. Y.; Kang, H. Y.; Sohn, H.; Oh, S.; Kim, J. Y.; Yoo, J. S.; Kim, Y. H.; Kim, C. H.; Jeon, J. H.; Lee, J. M.; Kang, H. A.; Miyoshi, E.; Taniguchi, N.; Yoo, H. S.; Ko, J. H. Functional proteomics study reveals that *N*-acetylglucosaminyltransferase V reinforces the invasive/metastatic potential of colon cancer through aberrant glycosylation on tissue inhibitor of metalloproteinase-1. *Mol. Cell Proteomics* **2008**, *7* (1), 1−14.

(13) Ahn, Y. H.; Lee, J. Y.; Kim, Y. S.; Ko, J. H.; Yoo, J. S. Quantitative analysis of an aberrant glycoform of TIMP1 from colon cancer serum by L-PHA-enrichment and SISCAPA with MRM mass spectrometry. *J. Proteome Res.* **2009**, *8* (9), 4216−24.

(14) Hammer, J. H.; Basse, L.; Svendsen, M. N.; Werther, K.; Brunner, N.; Christensen, I. J.; Nielson, H. J. Impact of elective resection on plasma TIMP-1 levels in patients with colon cancer. *Colorectal Dis.* **2006**, *8* (3), 168−72.

(15) Holten-Andersen, M. N.; Murphy, G.; Nielsen, H. J.; Pedersen, A. N.; Christensen, I. J.; Hoyer-Hansen, G.; Brunner, N.; Stephens, R. W. Quantitation of TIMP-1 in plasma of healthy blood donors and patients with advanced cancer. *Br. J. Cancer* **1999**, *80* (3−4), 495−503.

(16) Holten-Andersen, M. N.; Stephens, R. W.; Nielsen, H. J.; Murphy, G.; Christensen, I. J.; Stetler-Stevenson, W.; Brunner, N. High preoperative plasma tissue inhibitor of metalloproteinase-1 levels are associated with short survival of patients with colorectal cancer. *Clin. Cancer Res.* **2000**, *6* (11), 4292−9.

(17) Lee, S. J.; Yoo, H. J.; Bae, Y. S.; Kim, H. J.; Lee, S. T. TIMP-1 inhibits apoptosis in breast carcinoma cells via a pathway involving pertussis toxin-sensitive G protein and c-Src. *Biochem. Biophys. Res. Commun.* **2003**, *312* (4), 1196−201.

(18) Kim, H.; Lee, S. T. An intramolecular interaction between SH2-kinase linker and kinase domain is essential for the catalytic activity of protein-tyrosine kinase-6. *J. Biol. Chem.* **2005**, *280* (32), 28973−80.

(19) Lee, S. J.; Jang, J. W.; Kim, Y. M.; Lee, H. I.; Jeon, J. Y.; Kwon, Y. G.; Lee, S. T. Endostatin binds to the catalytic domain of matrix metalloproteinase-2. *FEBS Lett.* **2002**, *519* (1−3), 147−52.

(20) Kurschat, P.; Graeve, L.; Erren, A.; Gatsios, P.; Rose-John, S.; Roeb, E.; Tschesche, H.; Koj, A.; Heinrich, P. C. Expression of a biologically active murine tissue inhibitor of metalloproteinases-1 (TIMP-1) in baculovirus-infected insect cells. Purification and tissue distribution in the rat. *Eur. J. Biochem.* **1995**, *234* (2), 485−91.

(21) Ali, S.; Bassett, J. R. Studies on the role of glycosylation in the origin of the electrophoretic variants for rat corticosteroid-binding globulin. *Steroids* **1995**, *60* (11), 743−52.

(22) Koo, H. M.; Kim, J. H.; Hwang, I. K.; Lee, S. J.; Kim, T. H.; Rhee, K. H.; Lee, S. T. Refolding of the catalytic and hinge domains of human MT1-mMP expressed in *Escherichia coli* and its characterization. *Mol. Cells* **2002**, *13* (1), 118−24.

(23) Park, S. M.; Hwang, I. K.; Kim, S. Y.; Lee, S. J.; Park, K. S.; Lee, S. T. Characterization of plasma gelsolin as a substrate for matrix metalloproteinases. *Proteomics* **2006**, *6* (4), 1192−9.

(24) Laemmli, U. K. Cleavage of structural proteins during the assembly of the head of bacteriophage T4. *Nature* **1970**, *227* (5259), 680−5.

(25) Sung, J. Y.; Park, S. M.; Lee, C. H.; Um, J. W.; Lee, H. J.; Kim, J.; Oh, Y. J.; Lee, S. T.; Paik, S. R.; Chung, K. C. Proteolytic cleavage of extracellular secreted α-synuclein via matrix metalloproteinases. *J. Biol. Chem.* **2005**, *280* (26), 25216−24.

(26) Royle, L.; Radcliffe, C. M.; Dwek, R. A.; Rudd, P. M. Detailed structural analysis of N-glycans released from glycoproteins in SDS-PAGE gel bands using HPLC combined with exoglycosidase array digestions. *Methods Mol. Biol.* **2006**, *347*, 125−43.

(27) Bigge, J. C.; Patel, T. P.; Bruce, J. A.; Goulding, P. N.; Charles, S. M.; Parekh, R. B. Nonselective and efficient fluorescent labeling of glycans using 2-aminobenzamide and anthranilic acid. *Anal. Biochem.* **1995**, *230* (2), 229−38.

(28) Royle, L.; Campbell, M. P.; Radcliffe, C. M.; White, D. M.; Harvey, D. J.; Abrahams, J. L.; Kim, Y. G.; Henry, G. W.; Shadick, N. A.; Weinblatt, M. E.; Lee, D. M.; Rudd, P. M.; Dwek, R. A. HPLC-based analysis of serum N-glycans on a 96-well plate platform with dedicated database software. *Anal. Biochem.* **2008**, *376* (1), 1−12.

(29) Börnsen, K. O.; Mohr, M. D.; Widmer, H. M. Ion exchange and purification of carbohydrates on a Nafion(R) membrane as a new sample pretreatment for matrix-assisted laser desorption-ionization

mass spectrometry. *Rapid Commun. Mass Spectrom.* **1995**, *9* (11), 1031−1034.
(30) Harvey, D. J. Quantitative aspects of the matrix-assisted laser desorption mass spectrometry of complex oligosaccharides. *Rapid Commun. Mass Spectrom.* **1993**, *7* (7), 614−9.
(31) Jung, J. W.; Ji, A. R.; Lee, J.; Kim, U. J.; Lee, S. T. Organization of the human PTK7 gene encoding a receptor protein tyrosine kinase-like molecule and alternative splicing of its mRNA. *Biochim. Biophys. Acta* **2002**, *1579* (2−3), 153−63.
(32) Cailleau-Thomas, A.; Coullin, P.; Candelier, J. J.; Balanzino, L.; Mennesson, B.; Oriol, R.; Mollicone, R. FUT4 and FUT9 genes are expressed early in human embryogenesis. *Glycobiology* **2000**, *10* (8), 789−802.
(33) Natsuka, S.; Gersten, K. M.; Zenita, K.; Kannagi, R.; Lowe, J. B. Molecular cloning of a cDNA encoding a novel human leukocyte alpha-1,3-fucosyltransferase capable of synthesizing the sialyl Lewis x determinant. *J. Biol. Chem.* **1994**, *269* (24), 16789−16794.
(34) Yago, K.; Zenita, K.; Ginya, H.; Sawada, M.; Ohmori, K.; Okuma, M.; Kannagi, R.; Lowe, J. B. Expression of alpha-(1,3)-fucosyltransferases which synthesize sialyl Le(x) and sialyl Le(a), the carbohydrate ligands for E- and P-selectins, in human malignant cell lines. *Cancer Res.* **1993**, *53* (22), 5559−65.
(35) Kraulis, P. J. MOLSCRIPT: a program to produce both detailed and schematic plots of protein structures. *J. Appl. Crystallogr.* **1991**, *24*, 946−950.
(36) Gomis-Ruth, F. X.; Maskos, K.; Betz, M.; Bergner, A.; Huber, R.; Suzuki, K.; Yoshida, N.; Nagase, H.; Brew, K.; Bourenkov, G. P.; Bartunik, H.; Bode, W. Mechanism of inhibition of the human matrix metalloproteinase stromelysin-1 by TIMP-1. *Nature* **1997**, *389* (6646), 77−81.
(37) Berman, H. M.; Westbrook, J.; Feng, Z.; Gilliland, G.; Bhat, T. N.; Weissig, H.; Shindyalov, I. N.; Bourne, P. E. The Protein Data Bank. *Nucleic Acids Res.* **2000**, *28* (1), 235−42.
(38) Wormald, M. R.; Petrescu, A. J.; Pao, Y. L.; Glithero, A.; Elliott, T.; Dwek, R. A. Conformational studies of oligosaccharides and glycopeptides: complementarity of NMR, X-ray crystallography, and molecular modelling. *Chem. Rev.* **2002**, *102* (2), 371−86.
(39) Petrescu, A. J.; Milac, A. L.; Petrescu, S. M.; Dwek, R. A.; Wormald, M. R. Statistical analysis of the protein environment of N-glycosylation sites: implications for occupancy, structure, and folding. *Glycobiology* **2004**, *14* (2), 103−14.
(40) Murphy, G.; Willenbrock, F. Tissue inhibitors of matrix metalloendopeptidases. *Methods Enzymol.* **1995**, *248*, 496−510.
(41) d'Ortho, M. P.; Stanton, H.; Butler, M.; Atkinson, S. J.; Murphy, G.; Hembry, R. M. MT1-MMP on the cell surface causes focal degradation of gelatin films. *FEBS Lett.* **1998**, *421* (2), 159−64.
(42) Harvey, D. J. Fragmentation of negative ions from carbohydrates: part 1. Use of nitrate and other anionic adducts for the production of negative ion electrospray spectra from N-linked carbohydrates. *J. Am. Soc. Mass Spectrom.* **2005**, *16* (5), 622−30.
(43) Harvey, D. J. Fragmentation of negative ions from carbohydrates: part 2. Fragmentation of high-mannose N-linked glycans. *J. Am. Soc. Mass Spectrom.* **2005**, *16* (5), 631−46.
(44) Harvey, D. J. Fragmentation of negative ions from carbohydrates: part 3. Fragmentation of hybrid and complex N-linked glycans. *J. Am. Soc. Mass Spectrom.* **2005**, *16* (5), 647−59.
(45) Harvey, D. J.; Royle, L.; Radcliffe, C. M.; Rudd, P. M.; Dwek, R. A. Structural and quantitative analysis of N-linked glycans by matrix-assisted laser desorption ionization and negative ion nanospray mass spectrometry. *Anal. Biochem.* **2008**, *376* (1), 44−60.
(46) Yoshima, H.; Takasaki, S.; Ito-Mega, S.; Kobata, A. Purification of almond emulsin alpha-L-fucosidase I by affinity chromatography. *Arch. Biochem. Biophys.* **1979**, *194* (2), 394−8.
(47) Grabenhorst, E.; Nimtz, M.; Costa, J.; Conradt, H. S. In vivo specificity of human alpha1,3/4-fucosyltransferases III-VII in the biosynthesis of LewisX and Sialyl LewisX motifs on complex-type N-glycans. Coexpression studies from bhk-21 cells together with human beta-trace protein. *J. Biol. Chem.* **1998**, *273* (47), 30985−94.
(48) Kaneko, M.; Kudo, T.; Iwasaki, H.; Ikehara, Y.; Nishihara, S.; Nakagawa, S.; Sasaki, K.; Shiina, T.; Inoko, H.; Saitou, N.; Narimatsu, H. Alpha1,3-fucosyltransferase IX (Fuc-TIX) is very highly conserved between human and mouse; molecular cloning, characterization and tissue distribution of human Fuc-TIX. *FEBS Lett.* **1999**, *452* (3), 237−42.
(49) Struwe, W. B.; Cosgrave, E. F. J.; Byrne, J. C.; Saldova, R.; Rudd, P. M. Glycoproteomics in health and disease. In *Functional and Structural Proteomics of Glycoproteins*; Owens, R. J., Nettleship, J. E., Eds.; Springer: Dordrecht, Heidelberg, London, NY, 2011; pp 1−38.
(50) Dube, D. H.; Bertozzi, C. R. Glycans in cancer and inflammation—potential for therapeutics and diagnostics. *Nat. Rev. Drug Discovery* **2005**, *4* (6), 477−88.
(51) Hakomori, S. Glycosylation defining cancer malignancy: new wine in an old bottle. *Proc. Natl. Acad. Sci. U.S.A.* **2002**, *99* (16), 10231−3.
(52) Aarnoudse, C. A.; Garcia Vallejo, J. J.; Saeland, E.; van Kooyk, Y. Recognition of tumor glycans by antigen-presenting cells. *Curr. Opin. Immunol.* **2006**, *18* (1), 105−11.
(53) Miyoshi, E.; Moriwaki, K.; Nakagawa, T. Biological function of fucosylation in cancer biology. *J. Biochem.* **2008**, *143* (6), 725−9.
(54) Arnold, J. N.; Saldova, R.; Hamid, U. M.; Rudd, P. M. Evaluation of the serum N-linked glycome for the diagnosis of cancer and chronic inflammation. *Proteomics* **2008**, *8* (16), 3284−93.
(55) Saldova, R.; Wormald, M. R.; Dwek, R. A.; Rudd, P. M. Glycosylation changes on serum glycoproteins in ovarian cancer may contribute to disease pathogenesis. *Dis. Markers* **2008**, *25* (4−5), 219−32.
(56) Niemela, R.; Natunen, J.; Majuri, M. L.; Maaheimo, H.; Helin, J.; Lowe, J. B.; Renkonen, O.; Renkonen, R. Complementary acceptor and site specificities of Fuc-TIV and Fuc-TVII allow effective biosynthesis of sialyl-TriLex and related polylactosamines present on glycoprotein counterreceptors of selectins. *J. Biol. Chem.* **1998**, *273* (7), 4021−6.
(57) Nishihara, S.; Iwasaki, H.; Kaneko, M.; Tawada, A.; Ito, M.; Narimatsu, H. Alpha1,3-fucosyltransferase 9 (FUT9; Fuc-TIX) preferentially fucosylates the distal GlcNAc residue of polylactosamine chain while the other four alpha1,3FUT members preferentially fucosylate the inner GlcNAc residue. *FEBS Lett.* **1999**, *462* (3), 289−94.
(58) Taniguchi, N.; Honke, K.; Fukuda, M. *Handbook of Glycosyltransferases and Related Genes*; Tokyo-Berlin-Heidelberg-New York-London, 2002.
(59) Morrison, J. F.; Walsh, C. T. The behavior and significance of slow-binding enzyme inhibitors. *Adv. Enzymol. Relat. Areas Mol. Biol.* **1988**, *61*, 201−301.
(60) Van den Steen, P. E.; Opdenakker, G.; Wormald, M. R.; Dwek, R. A.; Rudd, P. M. Matrix remodelling enzymes, the protease cascade and glycosylation. *Biochim. Biophys. Acta* **2001**, *1528* (2−3), 61−73.
(61) Harvey, D. J.; Merry, A. H.; Royle, L.; Campbell, M. P.; Dwek, R. A.; Rudd, P. M. Proposal for a standard system for drawing structural diagrams of N- and O-linked carbohydrates and related compounds. *Proteomics* **2009**, *9* (15), 3796−801.